Sumer Journal for Pure Science (ISSN: 2790-7031)
SJPS 2023 (December), Vol. 2, No. 2, p.p.: 120-133

# Synthesis and Characterization of PMMA/$Bi_2O_3$-$Fe_2O_3$ Composites as Gamma Radiation Shielding

**Saleem M. Mahmood [1]*, Ali K. Aobiad [2], Mahdi M. Mutter [3]**

[1]*Department of Physics, College of Education for Pure Science, University of Anbar, Iraq*
[2]*Department of Physics, College of Education for Pure Science, University of Anbar, Iraq*
[3]*Centre of Apply Physics, Ministry of Science and Technology, Baghdad, Iraq*

**Abstract**

This article deals with the mechanical characteristics and hardness issues of PMMA sample that is based on various aspects related to radiation attenuation capability. Different doping is considered in this study namely nano bismuth trioxide ($Bi_2O_3$) and nano iron trioxide ($Fe_2O_3$) at doping concentrations of 0%, 0.5%, 1%, 3%, and 5%. Linear attenuation coefficient, absorptivity, and transmittance were ascertained using Bismuth-207 ($Bi^{207}$) and Cesium-137 ($Cs^{137}$) radioactive isotopes. The results demonstrate marked enhancements of hardness and radiation attenuating coefficients at higher doping levels notably at 5%. Furthermore, higher absorption values are associated with greater radiation effectiveness and more shield thickness and doping ratios. However, transmittance declines as the thickness of samples increases and the doping level rises. The results of these samples are quite encouraging and show the potential of being good radiation shielding materials; they have high linear attenuation coefficients.

**Keywords:** PMMA, Gamma radiation shielding, Linear Attenuation Coefficient, Nanoparticle doping, Radiation protection.

# تصنيع وتوصيف تركيبات PMMA/Bi2O3-Fe2O3 كمواد مركبة لتوفير درع لإشعاع كاما

**سليم محمد محمود[1]*, علي خلف عبيد[2], مهدي محمود مطر[3]**

[1]قسم الفيزياء, كلية التربية للعلوم الصرفة, جامعة الانبار, الانبار, العراق
[2] قسم الفيزياء, كلية التربية للعلوم الصرفة, جامعة الانبار, الانبار, العراق
[3]قسم تقنيات الطلاء, دائرة بحوث المواد , مركز الفيزياء التطبيقية , وزارة العلوم والتكنلوجيا, بغداد, العراق

**الخلاصة**

تتناول هذه المقالة الخصائص الميكانيكية وقضايا الصلابة لعينة *PMMA* التي تعتمد على جوانب مختلفة تتعلق بقدرة التوهين الإشعاعي. تم في هذه الدراسة أخذ شوائب مختلفة وهي ثالث أكسيد البزموت النانوي ($Bi_2O_3$) وثالث أكسيد الحديد النانوي ($Fe_2O_3$) عند تراكيز منشطات هي 0%، 0.5%، 1%، 3%، و5%. تم التحقق من معامل التوهين الخطي والامتصاصية والنفاذية باستخدام النظائر المشعة البزموت-207 ($Bi^{207}$) والسيزيوم-137 ($Cs^{137}$). أظهرت النتائج تحسينات ملحوظة في الصلابة ومعاملات تخفيف الإشعاع عند مستويات الشوائب الأعلى ولا سيما عند 5٪. علاوة على ذلك، ترتبط قيم الامتصاص الأعلى بزيادة فعالية الإشعاع وزيادة سماكة الدرع ونسب الشوائب. ومع ذلك، تنخفض النفاذية مع زيادة سمك العينات وارتفاع مستوى الشوائب. نتائج هذه العينات مشجعة للغاية وتظهر إمكانية كونها مواد جيدة للوقاية من الإشعاع؛ لديهم معاملات توهين خطية عالية.

* sel20u3009@uoanbar.edu.iq

## 1. Introduction

Undesirable exposure to high-energy radiation poses significant risks to both living organisms and inanimate structures. High-energy radiation plays a vital role in various fields, including nuclear industries, medicine, spacecraft, and agriculture, necessitating the implementation of rigorous radiation protection measures. Historically, lead has been a preferred choice for radiation shielding due to its high density, affordability, and effective radiation attenuation properties. It has been employed in various forms such as sheets, plates, foils, laminates, bricks, and blocks [1]. However, lead exhibits limitations in terms of versatility, chemical stability, mechanical strength, and inherent toxicity. In light of these shortcomings, extensive research efforts have been underway for the past few decades to identify alternative shielding materials capable of replacing lead. Polymer composites have emerged as a promising avenue in the realm of radiation protection. Researchers have explored diverse types of polymers as matrix materials, integrating various fillers as reinforcements tailored to their specific applications.

The use of nano-sized materials, for instance, Nano Bismuth Trioxide ($Bi_2O_3$), confers several benefits when used for radiation shielding in PMMA polymers. Nano-size particles have a larger surface area leading to high interaction with radiation, giving them better absorption and attenuation. Furthermore, they distribute more evenly in the polymer matrix and make sure that there are equal shielding properties. Another improvement in mechanical properties such as hardness and elasticity are ensured while keeping its transmittance intact through the introduction of nano-sized particles. This leads to exact control of particle size, which makes possible tuning of material characteristics for maximum absorption of radiation. At the nano-scale, quantum effects can further affect the electronic and optical properties, but since the structures are small, they can be compatible with a range of polymer matrixes maintaining the structure's strength at integration. The collective benefits of these nano-scale materials make them ideal for manufacturing better radiation shields in polymer composites.

Gwaily (2002) [2] conducted a study on the gamma attenuation properties of Galena-rubber composites exposed to 0.662 MeV gamma rays. The study reported a linear attenuation coefficient of 29.5 $m^{-1}$ and a half-value layer (HVL) of 0.023 m for the highest Galena-filled composite (500 phr). In a study by Korkut et al. (2013) [3], epoxy composites incorporating Ferrochromium slag were investigated for their radiation shielding effects against X-rays (85 keV), gamma rays (1250 keV), and neutrons (2–10 MeV). The research found that the inclusion of 50% FeCr slag in epoxy resin provided effective shielding, making it applicable in environments such as radiotherapy rooms, the nuclear industry, and containers for radioactive sources.

Furthermore, various researchers have explored the use of different matrices such as styrene-Polyaniline epoxy (Eid et al., 2013) [4] and (Hosseini et al., 2014) [5], coupled with metal or metal oxides as fillers, primarily focusing on attenuation studies. However, it is noteworthy that only a limited number of studies have delved into comprehending the structural, thermal, and mechanical stability of these composites. These aspects are crucial for the evaluation of any material as an efficient radiation shield.

In another investigation by Ambala et al. (2017) [6], polymer composites based on Isophthalic resin and filled with $Bi_2O_3$ were fabricated with varying weight percentages (0, 5, 10, 20, 30, 40, 50, and 60%). The results demonstrated enhanced shielding capabilities against $Cs^{137}$ gamma radiations, suggesting the potential of these composites as shielding materials, particularly for low dose rates.

Cao et al. (2020) [7] produced poly (methyl methacrylate) composites filled with Bi2O3 for shielding 0.662 MeV gamma rays, yielding a linear attenuation coefficient of 0.206 $cm^{-1}$ for the 50 wt% Bi2O3 composites. Their work compared the shielding performance of these composites with conventional materials and demonstrated favorable shielding properties, especially for lower and medium gamma energies.

## 2. Experiments

### 2.1. Materials

Poly(methyl methacrylate) (PMMA) is a transparent, colorless polymer with a molecular formula of ($C_5H_9O_2$) and a density of 1.19 g/$cm^3$ [8]. It belongs to the category of thermoplastic polymers and is used as a base material for preparing polymeric composite materials. PMMA is manufactured by the company Ottobock. This polymer undergoes a transition from a liquid to a solid state when a hardening agent, Benzoyl Peroxide, is added. The hardening agent is in the form of white powder and is added to PMMA in a ratio of 1:100.

### 2.2. Preparation of polymer composites

To prepare a 100g sample of pure PMMA polymer, 100g of the polymer is carefully weighed using an electronic balance. Subsequently, 1g of the hardening agent, specifically Benzoyl Peroxide from Central Drug House (CDH), is added to the PMMA at room temperature in a precise 1:100 ratio. The mixture is then meticulously blended using a mechanical mixer for a duration ranging between 25 to 30 minutes, ensuring the achievement of homogeneity.

For the preparation of nano-composite samples comprising PMMA/$Fe_2O_3$/$Bi_2O_3$, an appropriate quantity of PMMA polymer is weighed. Following this, the required amount of nano iron oxide and nano bismuth oxide, each in proportions of (0.5, 1, 3, 5) by weight and with a 1:1 ratio, is carefully weighed according to the desired weight fraction for each sample. The blending process is conducted meticulously in an electric mixer for one hour, aimed at achieving a homogeneous mixture. Subsequently, the mixture undergoes a 30-minute treatment on a vibrating apparatus to eliminate bubbles and ensure uniformity. Following this, the hardening agent is introduced at a precise 1:100 ratio. The mixer continues to operate for a duration ranging from 3 to 5 minutes, during which a rise in the composite's temperature signifies the initiation of the reaction among its constituents.

The samples are left undisturbed within the molds for 24 hours, allowing them to fully solidify. After this curing period, the samples are carefully extracted from the molds.

### 2.3. Characterization

#### 2.3.1 Scanning electron microscope

Scanning Electron Microscope (SEM) images were employed to investigate the shape and distribution of ($Bi_2O_3$: $Fe_2O_3$) particles within the interstitial spaces of the PMMA polymer and its forms (1-a, b, c, d, and e). The SEM images reveal that the particles are unevenly distributed within the matrix with an appropriate dispersion. The doping materials ($Bi_2O_3$: $Fe_2O_3$) tend to aggregate at one or more points along the radial fronts, adjacent to the edge pathways, which could potentially result in crack propagation. Furthermore, it has been observed that the protrusions became less pronounced as the loading of the particles increased, attributed to the reduction in sample stress, resulting in a smoother surface. The particle size for all samples (276.655, 260, 394.67, 312.465, 551.67) nanometers for PMMA with the addition of (0, 0.5, 1, 3, 5) % of ($Bi_2O_3$: $Fe_2O_3$), respectively. The resin's positioning within PMMA within the agglomerations of the added materials was also confirmed. Additionally, larger particle agglomerations of ($Bi_2O_3$: $Fe_2O_3$) were observed in form (1-e) for composites with a 5% filler ratio, but these should be minimized to ensure proper functionality [6].

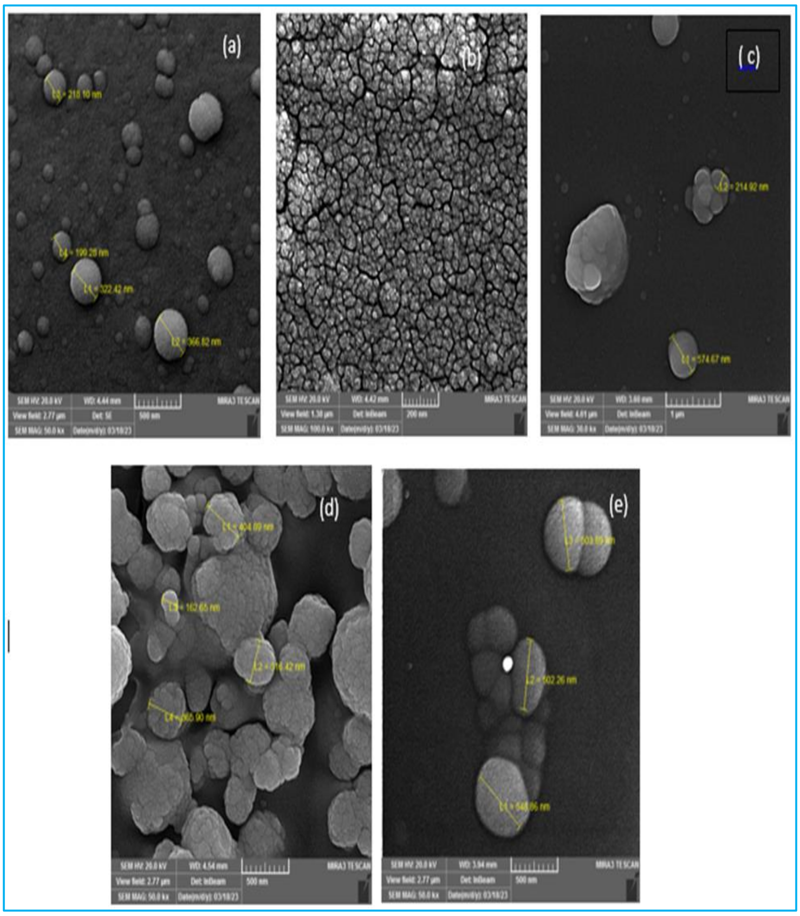


**Figure -1** shows electron microscope images of samples prepared from PMMA:($Bi_2O_3$:$Fe_2O_3$).

## 2.4. Gamma shielding

Experiments were conducted to shield against gamma radiation, utilizing gamma radiation sources, namely, the highly radioactive cesium source $Cs^{137}$ (with an activity of 4.5 µCi), emitting gamma rays with a high intensity of 48, and the bismuth source $Bi^{207}$ (with an activity of 10 µCi) and an intensity of 122. The exposure time of the samples to gamma radiation was 60 seconds. The sources were placed in front of a lead block, and the radiation exited through an aperture onto the sample. The amount of transmitted radiation, represented as (I), was measured using a Geiger counter.

In this study, various doping percentages were considered, including 5%, 3%, 1%, and 0.5%. These doping ratios were equivalent for both nano iron oxide and nano bismuth oxide. The weight of the PMMA polymer and the nano oxides was 100 grams. Four samples were prepared accordingly.

The linear attenuation coefficient was determined as a function of thickness [9].

$$I = I_{\circ} e^{-\mu x} \qquad (1)$$

$I_o$ represents the intensity of the source, $I$ is the transmitted radiation intensity, $x$ denotes the sample thickness, and $\mu$ is the linear attenuation coefficient. The transmittance factor was calculated using the following equation [10]

$$T = \frac{I}{I_\circ} \quad (2)$$

Similarly, absorptivity was calculated using the equation

$$A = -log\frac{I}{I_\circ} \quad (3)$$

### 2.5. Hardness test

All samples were subjected to hardness tests based on the Shore D procedure. It is based on a manual instrument with the needle spring device used to puncture the sample surface. When the needle punctures the surface of the sample, a reading shows up onto the device screen denoting the hardness of the sample at that point. Readings were taken from five regions of each sample taken. Then, the mean of these readings was determined.

## 3. Results and discussion

### 3.1. Hardness Test results

The hardness test is based on the amount of penetration and deformation that occur in a material when exposed to an external load. Table 1 shows how the Shore D hardness test was performed on the nano-composites samples.

**Table 1** presents the nano-composite hardness values.

| Impregnation ratio | Nano composites % | | | Hardness (Shore D) |
|---|---|---|---|---|
| | PMMA | $Fe_2O_3$ | $Bi_2O_3$ | |
| 0 | 6 | 0 | 0 | 71.6 |
| 0.5 % | 5..97 | 0.015 | 0.015 | 73.4 |
| 1 % | 5.94 | 0.03 | 0.03 | 79 |
| 3% | 5.82 | 0.09 | 0.09 | 83.6 |
| 5% | 5.7 | 0.15 | 0.15 | 89 |

This test showed an increase in hardness of nano iron oxide and nano bismuth oxide doped samples as a function of doping percentage. The higher the value of hardness is associated with reinforcing oxides being present within PMMA and not PMMA itself. Also, hardness is greatly depending on molecular bonding strength, types of surface, and temperature in Figure 2. This is similar to other studies, which witnessed enhancement in hardness[11].

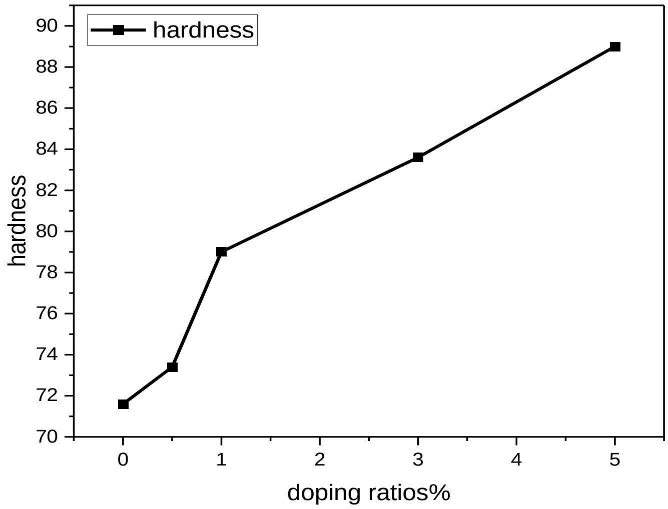


**Figure - 2** illustrates the hardness as a function of doping percentages.

### 3.2. Radiological tests

Polymeric materials have been increasingly utilized in recent years for protection against harmful nuclear radiation. These materials have been developed by incorporating them with specific ratios of nano bismuth oxide and nano iron oxide to mitigate nuclear radiation. Among the most important tests conducted for attenuating gamma rays emitted from cesium-137 (with an intensity of 48) and bismuth-207 (with an intensity of 122) sources.

**Table 2.** illustrates the values of transmitted and absorbed radiation as a function of sample thickness (mm).

| Sample name | Thickness (mm) | $Cs^{137}$ Source, 4.5 μc | | | $Bi^{207}$ Source, 10μc, | | |
|---|---|---|---|---|---|---|---|
| | | I | $I/I_o$ | $\log I/I_o$ | I | I/Io | $\log I/I_o$ |
| **PMMA pure** | 0 | 48 | 1 | 0 | 122 | 1 | 0 |
| | 8 | 32 | 0.666 | -0.1765 | 56 | 0.459 | -0.3381 |
| | 16 | 30 | 0.625 | -0.2041 | 50 | 0.409 | -0.3882 |
| | 24 | 28 | 0.583 | -0.2343 | 47.5 | 0.389 | -0.4100 |
| | 32 | 24 | 0.50 | -0.3010 | 44 | 0.360 | -0.4436 |
| **0.5% ($Bi_2O_3$:$Fe_2O_3$)** | 8 | 30 | 0.625 | -0.2041 | 47.5 | 0.389 | -0.4100 |
| | 16 | 27 | 0.562 | -0.2502 | 42 | 0.344 | -0.4634 |
| | 24 | 23 | 0.479 | -0.3196 | 40 | 0.327 | -0.4854 |
| | 32 | 19 | 0.395 | -0.4034 | 36 | 0.295 | -0.5301 |
| **1% ( $Bi_2O_3$:$Fe_2O_3$)** | 8 | 28 | 0.583 | -0.2343 | 44 | 0.360 | -0.4436 |
| | 16 | 25 | 0.520 | -0.2839 | 40 | 0.327 | -0.4854 |
| | 24 | 22 | 0.458 | -0.3391 | 35 | 0.286 | -0.5436 |
| | 32 | 18 | 0.375 | -0.4259 | 31 | 0.254 | -0.5951 |
| **3% ( $Bi_2O_3$:$Fe_2O_3$)** | 8 | 26 | 0.541 | -0.2668 | 39 | 0.319 | -0.4962 |
| | 16 | 24 | 0.5 | -0.3010 | 37 | 0.303 | -0.5185 |
| | 24 | 21 | 0.437 | -0.3595 | 34 | 0.278 | -0.5559 |
| | 32 | 17 | 0.354 | -0.4509 | 29 | 0.237 | -0.6252 |
| **5% ( $Bi_2O_3$:$Fe_2O_3$)** | 8 | 22 | 0.458 | -0.3391 | 31 | 0.254 | -0.5951 |
| | 16 | 20 | 0.416 | -0.3809 | 28 | 0.229 | -0.6401 |
| | 24 | 17 | 0.354 | -0.4509 | 23 | 0.188 | -0.7258 |
| | 32 | 14 | 0.291 | -0.5361 | 19 | 0.155 | -0.8096 |

### 3.2.1. Radioactive transmittance

The study of radiation penetration is crucial in determining and studying the attenuation of prepared shields. In this project, Equation (3) was used to calculate the intensity of incident and transmitted radiation for cesium-137 (Cs-137) sources (with an activity of 4.5 μCi) and bismuth-207 (Bi-207) sources (with an activity of 10 μCi) as a function of the thickness of the protective shield made of polymethyl methacrylate (PMMA) doped with a composite of bismuth trioxide and iron trioxide (Bi2O3:Fe2O3).

From Table 2, the values of incident and transmitted intensities from both sources were represented as a function of the prepared shield thickness. Figure (3) illustrates the relationship between transmittance and thickness for the cesium source. It is evident that the relationship between transmittance and shield thickness is an inverse one, where transmittance decreases with an increase in thickness and doping ratios. The highest transmittance was observed at 0.666 for the pure PMMA sample, while the lowest transmittance was for the 5% doped sample at 0.291.

Figure (4) demonstrates the linear relationship between incident and transmitted intensities for the same thicknesses for the bismuth source. It is noticeable that these results exhibit the same behavior as the cesium-137 source, with the highest transmittance being 0.459 for the undoped sample and the lowest transmittance being 0.155 for the 5% doped sample.

It is observed that the lowest transmittance was recorded for the 5% doped sample, as the oxides used have good attenuation capability for gamma radiation [1, 12]. These findings are consistent with the results obtained by previous researchers [13, 14].

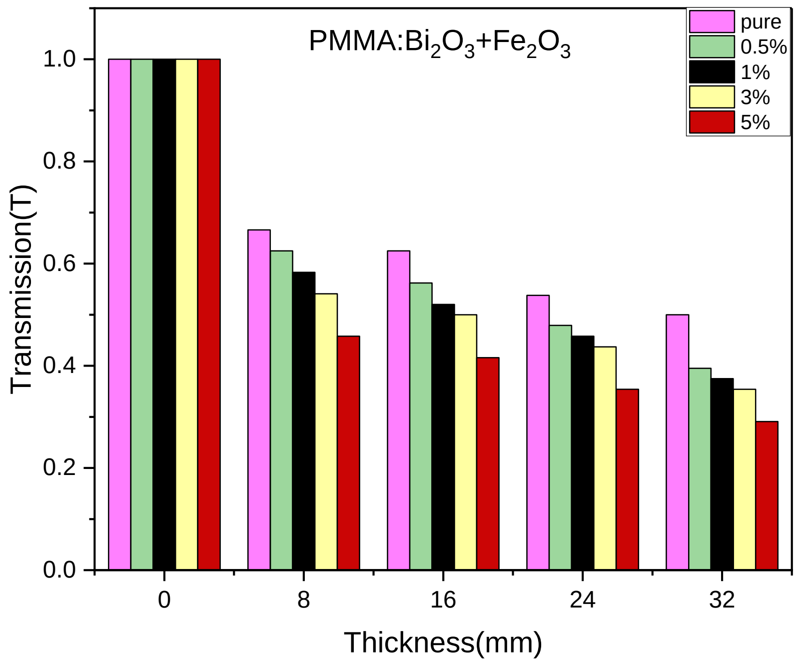


**Figure - 3.** illustrates the transmittance factor for the cesium-137 (Cs-137) source as a function of thickness.

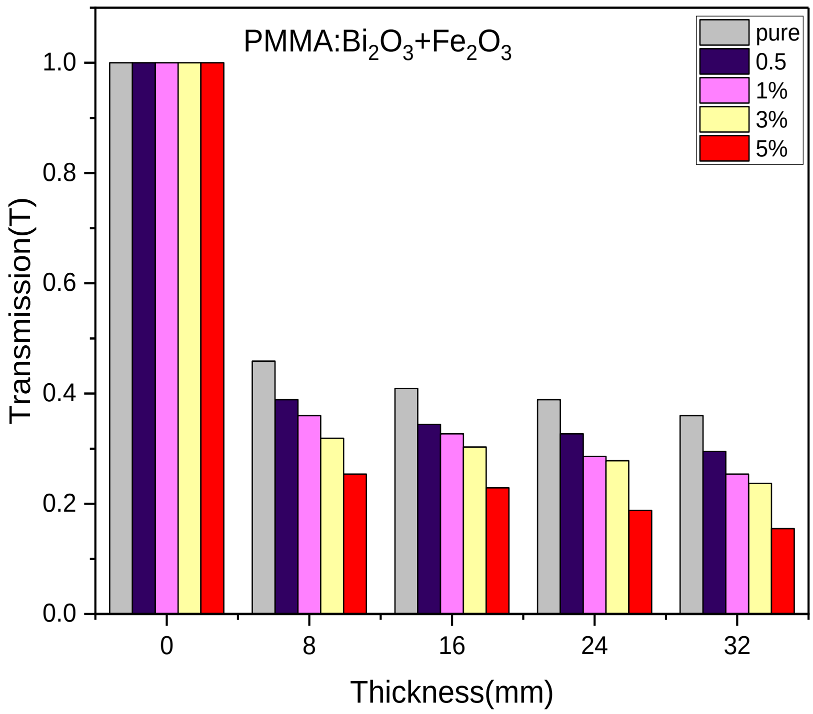


**Figure - 4.** represents the transmittance factor as a function of shield thickness for the prepared samples for the bismuth-207 (Bi-207) source.

### 3.2.2. Radioactive absorbency

The absorbance is considered an important variable in characterizing radiation shields, and the absorbance values, as calculated and presented in Table 2, were obtained using Equation (3). These values were calculated for both cesium-137 and bismuth-207 sources as functions of shield thickness. The results are depicted in Figures (3) and.(4)

Figure (5) shows that the highest absorbance was achieved by the prepared and 5% doped sample, with a value of 0.55 at a thickness of 8 mm. The lowest absorbance was observed for the pure sample, with a value of 0.1857. The absorbance for all prepared samples increased with increasing thickness and doping ratios.

Figure (6), for the bismuth-207 radioactive source, exhibited a similar behavior to the prepared samples using the cesium-137 source. The highest absorbance was recorded at 0.5951 for the 5% doped sample at a thickness of 8 mm, while the lowest absorbance was observed for the pure sample, with a value of 0.3381 at the same thickness. These results are in accordance with the findings of a previous researcher [15].

Additionally, from these two figures, the behavior of absorbance for the prepared shields with varying doping ratios was studied. It was observed that absorbance increased with increasing doping ratios for all thicknesses and for both radioactive sources. This suggests the effectiveness and adaptability of shield additives in attenuating radiation. This behavior aligns with the relationship between absorbance, thickness, and density.

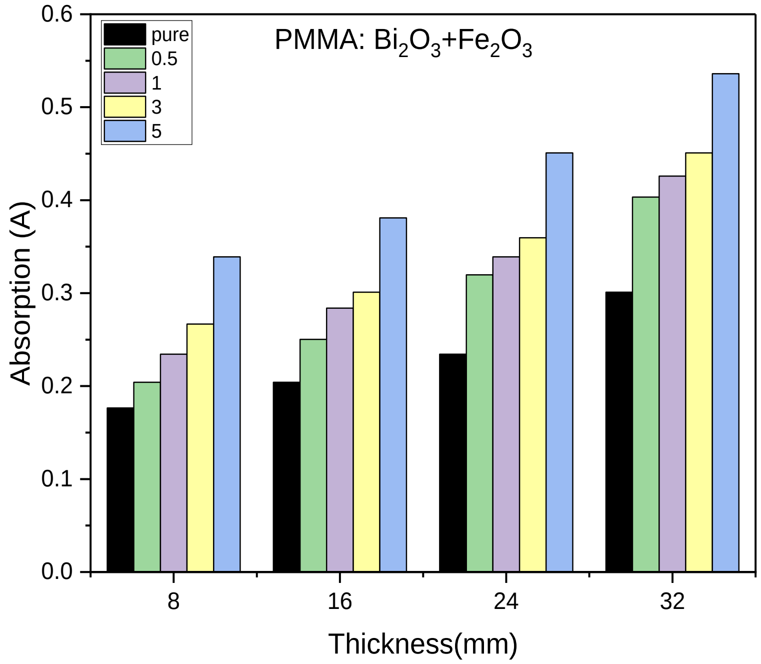


**Figure - 5.** illustrates the absorption coefficient as a function of thickness for the cesium-137 (Cs-137) source.

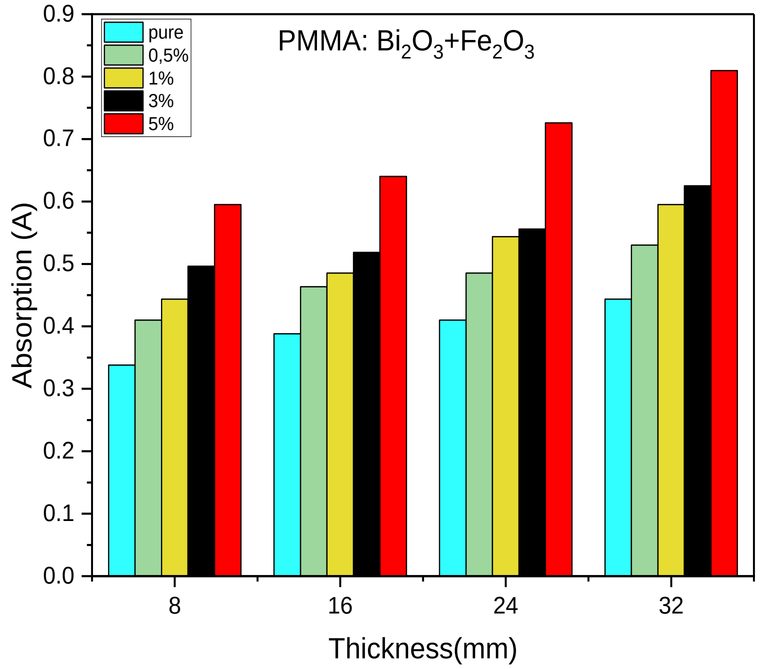


**Figure - 6.** represents the absorption coefficient as a function of shield thickness for the samples prepared for the bismuth-207 (Bi-207) source.

Figures (5) and (6) illustrate the relationship between absorption coefficients and the sample or shield density. It can be observed from the Figures, which represent the two radiation sources used in this study, that the absorption coefficients increase with the increase in shield density due to the higher doping ratios at a selected thickness, which is 8 mm in this case. These results indicate that a significant portion of the incident radiation is absorbed by the shielding materials, especially the additives. This behavior aligns with many previous studies in this field [16].

### 3.2.3. Linear Attenuation Coefficient (μ)

The values of the linear attenuation coefficient (μ) were determined for both cesium-137 ($Cs^{137}$) and bismuth-207 ($Bi^{207}$) sources for the samples prepared from polymethyl methacrylate (PMMA) with different doping ratios (5%, 3%, 1%, 0.5%, 0%) of the ($Bi_2O_3$:$Fe_2O_3$) nanocomposite, as shown in Table (3). The relationship between Ln(I/Io) as a function of the sample thickness was plotted for both sources. These experimental results provide the linear attenuation coefficient as a function of the thickness of the shields used for the $Cs^{137}$ and $Bi^{207}$ sources.

**Table 3.** presents the experimental results for the linear attenuation coefficient (μ) in $mm^{-1}$ for the prepared models with different doping ratios.

| Sample name | Thickness (mm) | $Cs^{137}$ Source, 4.5 μc | | $Bi^{207}$ Source, 10μc, | |
|---|---|---|---|---|---|
| | | μ($mm^{-1}$) | μ($mm^{1}$)/sample | μ($mm^{-1}$) | μ($mm^{-1}$)/sample |
| **PMMA pure** | 8 | 0.050 | 0.030 | 0.097 | 0.055 |
| | 16 | 0.029 | | 0.055 | |
| | 24 | 0.022 | | 0.039 | |
| | 32 | 0.021 | | 0.031 | |
| **0.5% ($Bi_2O_3$:$Fe_2O_3$)** | 8 | 0.058 | 0.038 | 0.118 | 0.067 |
| | 16 | 0.036 | | 0.066 | |
| | 24 | 0.030 | | 0.046 | |
| | 32 | 0.029 | | 0.038 | |
| **1% ( $Bi_2O_3$:$Fe_2O_3$)** | 8 | 0.067 | 0.042 | 0.127 | 0.072 |
| | 16 | 0.040 | | 0.069 | |
| | 24 | 0.032 | | 0.052 | |
| | 32 | 0.030 | | 0.042 | |
| **3% ( $Bi_2O_3$:$Fe_2O_3$)** | 8 | 0.076 | 0.046 | 0.142 | 0.078 |
| | 16 | 0.043 | | 0.074 | |
| | 24 | 0.034 | | 0.053 | |
| | 32 | 0.032 | | 0.044 | |
| **5% ( $Bi_2O_3$:$Fe_2O_3$)** | 8 | 0.097 | 0.058 | 0.171 | 0.097 |
| | 16 | 0.054 | | 0.092 | |
| | 24 | 0.043 | | 0.069 | |
| | 32 | 0.038 | | 0.058 | |

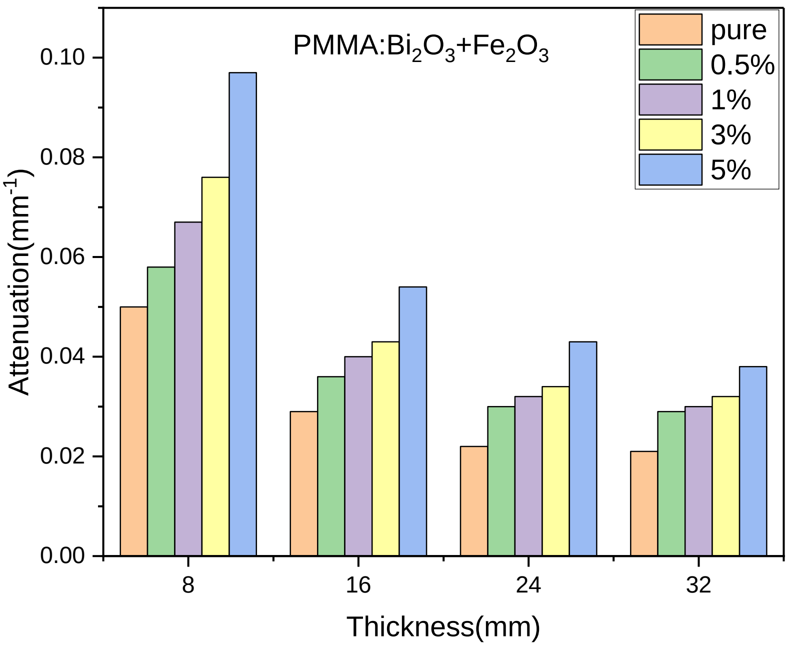


**Figure -7.** illustrates the linear attenuation coefficient (μ) for each thickness of the samples with various doping ratios, using the Cs137 source.

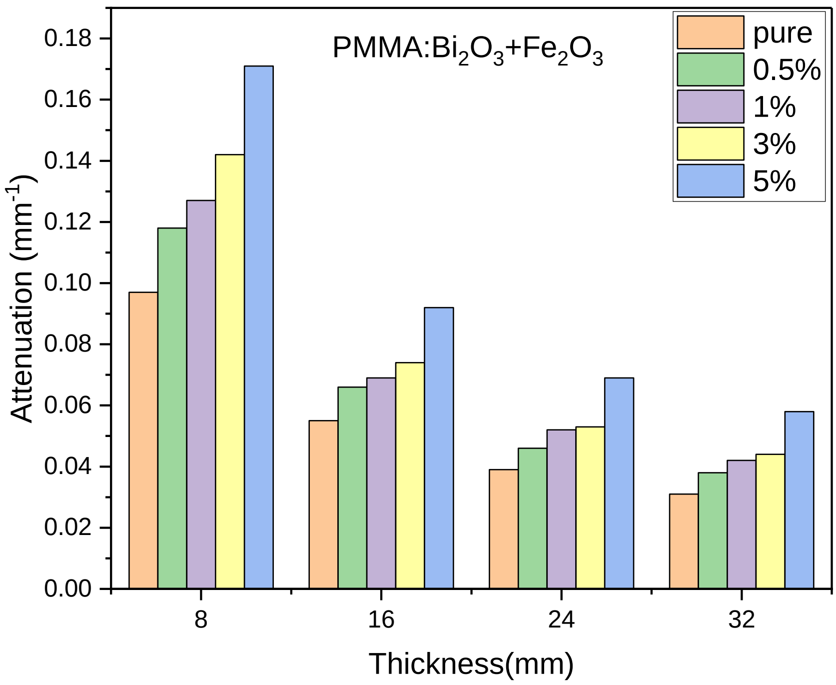


**Figure - 8.** shows the linear attenuation coefficient (μ) for each thickness of the samples with various doping ratios for the $Bi^{207}$ source.

The Figure (9) illustrates the relationship between linear attenuation and doping ratios using both cesium and bismuth sources. It is evident from the graph that linear attenuation increases with higher concentrations of bismuth and iron, with the greatest effect observed for the bismuth source due to its higher radioactivity compared to the cesium $CS^{137}$ source

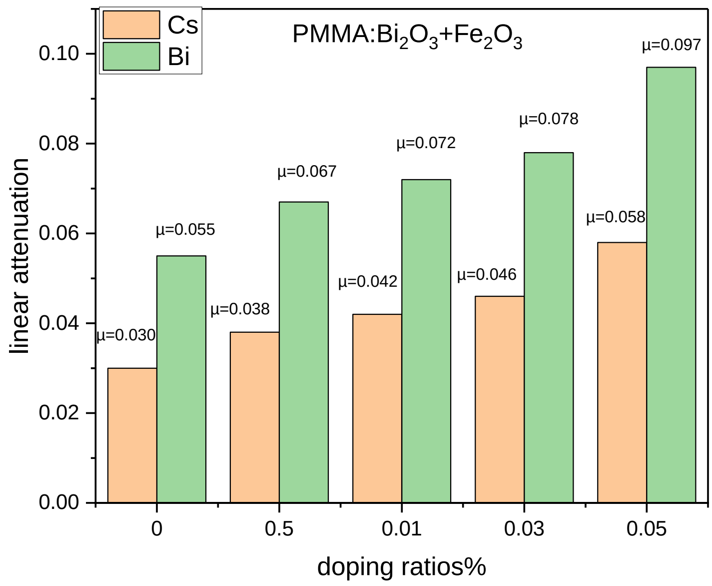


**Figure - 9.** illustrates the relationship between the doping ratio and linear attenuation for both the cesium $Cs^{137}$ and bismuth $Bi^{207}$ sources

## 4. Conclusions

In conclusion, this study investigated the radiation attenuation properties of polymethyl methacrylate (PMMA) when doped with nano-oxides, specifically iron oxide ($Fe_2O_3$) and bismuth oxide ($Bi_2O_3$), at varying doping ratios of 5%, 3%, 1%, and 0.5%. The findings of this research reveal several significant outcomes: (1) The addition of nano-oxides led to a notable increase in the hardness of PMMA, with the most substantial improvement observed at a 5% doping ratio. This enhancement suggests that nano-oxide reinforcement positively impacts the mechanical properties of PMMA. (2) The study showed that radiation permeability, representing the intensity of transmitted gamma rays through shielding materials, decreased with increased sample thickness and doping ratios. Notably, the most effective attenuation was achieved with a 5% nano-oxide doping ratio. (3) The linear attenuation coefficient (μ) exhibited an upward trend with increasing sample thickness and doping ratio for all composite samples, indicating improved radiation attenuation capabilities. (4) The absorption coefficient (A) increased proportionally with sample thickness and the addition of nano-oxides, emphasizing the effective absorption of ionizing radiation. (5) Among the various doping ratios studied, the 5% doping ratio of nano-oxides ($Fe_2O_3$ + $Bi_2O_3$) was identified as the most effective configuration for radiation attenuation in PMMA, thus representing an optimal choice for radiation shielding applications. These findings signify the potential utility of nano-oxide-doped PMMA as a robust radiation shielding material, particularly when configured with a 5% doping ratio. Moreover, this study contributes to the growing body of knowledge in the field of radiation shielding materials. Further research avenues may explore practical applications and address any limitations encountered during this investigation. It is essential to acknowledge that this study provides valuable insights into radiation attenuation but may have its own constraints and limitations that warrant consideration in future research endeavors.

## References

1. Fontainha, C.C., A.T. Baptista Neto, and L.O. Faria, *Radiation shielding with Bi 2 O 3 and ZrO 2: Y composites: preparation and characterization.* 2015. Available from: https://inis.iaea.org/search/search.aspx?orig_q=RN:46135938.
2. Gwaily, S., *Galena/(NR+ SBR) rubber composites as gamma radiation shields.* Polymer testing, 2002. **21**(8): p. 883-887 DOI: https://doi.org/10.1016/S0142-9418(02)00023-5
3. Korkut, T., et al., *X-ray, gamma, and neutron radiation tests on epoxy-ferrochromium slag composites by experiments and Monte Carlo simulations.* International journal of polymer analysis and characterization, 2013. **18**(3): p. 224-231 DOI: https://doi.org/10.1080/1023666X.2013.755658.
4. Eid, G.A., et al., *Application of epoxy/Pb3O4 composite for gamma ray shielding.* Arab. J. Nucl. Sci. Appl, 2013. **46**(2): p. 226-233. Available from: https://www.semanticscholar.org/paper/Application-of-Epoxy-Pb3O4-Composite-for-Gamma-Ray-Eid-Kany/a249f9bd72f53b1fe019f1fa4bd1eb7c1814f198.
5. Hosseini, S.H., M. Askari, and S.N. Ezzati, *X-ray attenuating nanocomposite based on polyaniline using Pb nanoparticles.* Synthetic metals, 2014. **196**: p. 68-75 DOI: https://doi.org/10.1016/j.synthmet.2014.07.015.
6. Ambika, M., et al., *Preparation and characterisation of Isophthalic-Bi2O3 polymer composite gamma radiation shields.* Radiation Physics and Chemistry, 2017. **130**: p. 351-358 DOI: https://doi.org/10.1016/j.radphyschem.2016.09.022.
7. Cao, D., et al., *Gamma radiation shielding properties of poly (methyl methacrylate)/Bi2O3 composites.* Nuclear Engineering and Technology, 2020. **52**(11): p. 2613-2619 DOI: https://doi.org/10.1016/j.net.2020.04.026.
8. Monem, Z.M.A., Q.A. Hamad, and J.K. Oleiwi, *DENSITY AND WATER ABSORPTION PROPERTIES OF PMMA REINFORCED BY PEANUT AND WALNUT SHELLS POWDERS USED IN DENTAL APPLICATIONS.* THE IRAQI JOURNAL FOR MECHANICAL AND MATERIALS ENGINEERING, 2021. **21**(1): p. 46-53 DOI: https://doi.org/10.32852/iqjfmme.v21i1.538.
9. Goldstein, J.I., et al., *Scanning electron microscopy and X-ray microanalysis*. 2017: springer.
10. S Faiq, L. and Z. F Attiyah, *The Effect of Ferrite Content on the Thermomechanical and Dielectric Strength Properties of Epoxy Composite.* Engineering and Technology Journal, 2016. **34**(1): p. 186-192. Available from: https://www.iasj.net/iasj/download/2dc54dfadc38a04f.
11. Crawford, R.J. and P.J. Martin, *Plastics engineering*. 2020: Butterworth-Heinemann.
12. Sayyed, M., et al., *Recycling and optimizing waste lab glass with Bi2O3 nanoparticles to use as a transparent shield for photons.* Journal of Materials Research and Technology, 2022. **17**: p. 2073-2083 DOI: https://doi.org/10.1016/j.jmrt.2022.01.113.
13. Alhammashi, M.A., H.D. ALattabi, and M.J. Aldhuhaibat. *Improving the attenuation Ability of gamma rays for silicate glass system composites (GS-PbO): a comparative*

*theoretical study*. in *IOP Conference Series: Materials Science and Engineering*. 2020. IOP Publishing DOI: https://doi.org/10.1088/1757-899X/928/7/072077.

14. Mehranpour, S., *Comparison of beta, neutron and gamma attenuation properties of pmma/colemanite composites*. 2019, Energy Institute.
15. Husain, H., N.R. Naji, and B. Mahmood. *Investigation of gamma ray shielding by polymer composites*. in *IOP Conference Series: Materials Science and Engineering*. 2018. IOP Publishing DOI: https://doi.org/10.1088/1757-899X/454/1/012131.
16. Aowd, N.M. and H.S. Hussain, *Absorption coefficient measurement of bremsstrahlung radiation in nano composite.* Engineering and Technology Journal, 2015. **33**(7 Part (B) Scientific). Available from: https://www.iasj.net/iasj/download/5fd6f0683d36a6d6.